

An Efficient and Practical Decoupling Feeding Network for Antenna Phased Arrays

R. Shavit, *Senior Member, IEEE*, and E. Rivkin

Abstract—A new approach to design decoupling feeding networks for large antenna phased arrays is proposed. The approach is based on a combination of two existing methods, resulting in significant hardware savings. The decoupling network allows matching each of the input ports individually and independently of the excitation. A genetic algorithm was used to change the values of the components for optimum performance in case the decoupling network is lossy.

Index Terms—Antenna arrays, decoupling, impedance matrix.

I. INTRODUCTION

OVER the years, the use of antenna arrays increased in various areas (such as communication, biomedicine, radars, etc.). One of the major problems in antenna phased arrays is coupling among the elements, which causes difficulties in matching the system for different predefined radiation patterns. The active impedance at each port depends on the input currents, and different matching networks are required for every excitation.

There are two main approaches to deal with the problem. The first one is based on reducing the mutual coupling using preliminary measures and calculations, leading to compensation for the mutual coupling effect in the antenna array [1]. The second one is based on designing a feeding network connected to the antenna array, such that its input ports are decoupled and can be matched independently of the excitation [2], [3].

In this letter, the second approach is chosen. The theoretical basis for the proposed solution is the eigenmode theory [2], leading to a network that excites the eigenmodes of the array and decouples the ports. Hardware implementation of the decoupling network (DN) was examined for an array of 2×4 dipoles above a large ground plane and is based on a combination of the two methods [2] and [3]. Both methods use directional couplers for implementation. The first method uses symmetries in the array and performs decoupling in stages. The second method is a general one, but requires a large number of couplers. The benefits of the combination between the methods are significant hardware savings as will be described.

II. PROBLEM FORMULATION

The problem of mutual coupling arises in antenna arrays due to small distances between the radiating elements, resulting in dependence between the ports' currents I_i and voltages V_i .

Manuscript received September 18, 2010; accepted October 05, 2010. Date of publication October 11, 2010; date of current version October 25, 2010.

The authors are with the Department of Electrical and Computer Engineering, Ben Gurion University of the Negev, Beer-Sheva 84105, Israel (e-mail: rshavit@ee.bgu.ac.il; rivkine@ee.bgu.ac.il).

Color versions of one or more of the figures in this letter are available online at <http://ieeexplore.ieee.org>.

Digital Object Identifier 10.1109/LAWP.2010.2086425

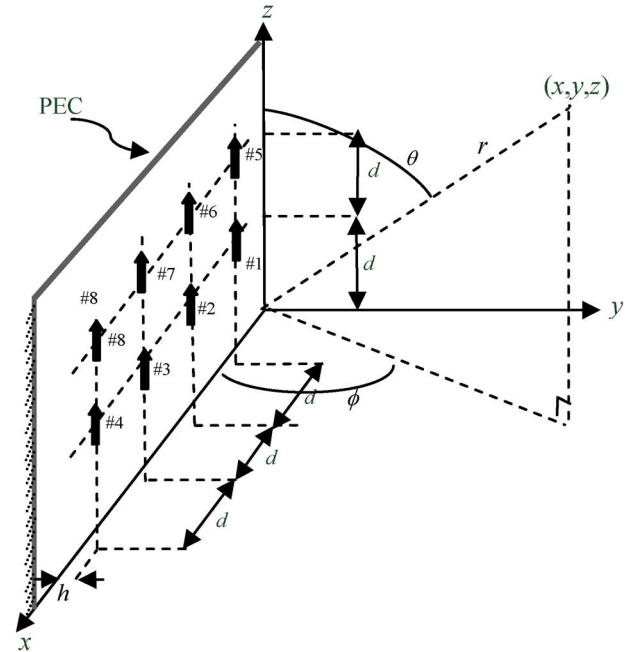


Fig. 1. The geometry of a 2×4 dipole array above a large ground plane.

This effect can be described for an M -elements array through the impedance matrix $[Z]$, with $Z_{i,j}$ representing the coupling between the i and j elements. Accordingly, the active impedance at the i th port is given by

$$\begin{aligned} Z_i^a &= \frac{V_i}{I_i} \\ &= \frac{I_1}{I_i} Z_{i,1} + \frac{I_2}{I_i} Z_{i,2} + \dots + \frac{I_{i-1}}{I_i} Z_{i,i-1} + Z_{i,i} \\ &\quad + \frac{I_{i+1}}{I_i} Z_{i,i+1} + \dots + \frac{I_M}{I_i} Z_{i,M}. \end{aligned} \quad (1)$$

As one can notice, the active impedance (and therefore, the active reflection coefficient) at each port depends on the input currents, leading to significant power mismatch. The problem becomes acute for phased arrays, where the phases of the currents always change. This coupling might produce blind spots in the phased array radiation pattern.

In this letter, without loss of generality, we chose to examine the effect of mutual coupling and search for a solution to the problem for an array of 2×4 dipoles above a large ground plane. Due to its simplicity, the $[Z]$ matrix of such an array can be easily calculated with no need of using advanced numerical methods. The suggested array geometry is shown in Fig. 1.

Such an array has a full 8×8 $[Z]$ (and $[S]$) matrix, where all of its elements can be calculated using the reciprocity theorem and the analytical expressions of the near field of a dipole [4]. Mathematically, the main goal is to transform the full $[Z]$ (or $[S]$) matrix

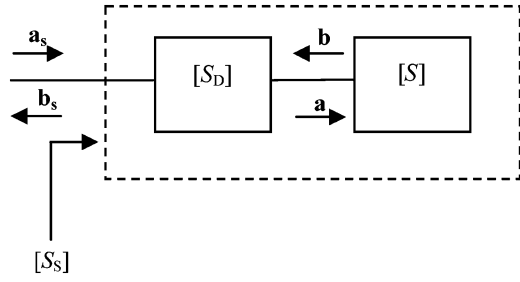


Fig. 2. Schematic drawing of the system, which includes the antenna array $[S]$ and the decoupling network $[S_D]$.

to a diagonal $[Z_s]$ (or $[S_s]$) matrix through an additional network connected to the antenna array, such that $[Z_s]$ is the impedance matrix of the whole system and $[S_s]$ is its corresponding scattering matrix. Once the system matrix is diagonal, matching is possible at each port independently of other ports.

The diagonalization of the impedance matrix $[Z_s]$ is obtained using the eigenmode theory, as described in [2]. The $2M$ port schematic decoupling network connected to the antenna array (described also by the scattering matrix $[S_D]$) is shown in Fig. 2. One of the design considerations of the decoupling network is the requirement that its inputs and outputs should be matched for efficient power transmission to the antenna array elements.

This implies that the structure of $[S_D]$ should be

$$[S_D] = \begin{pmatrix} [0] & [S_{D,21}]^T \\ [S_{D,21}] & [0] \end{pmatrix}. \quad (2)$$

Applying network relations and using (2) leads to

$$[S_s] = [S_{D,21}]^T [S] [S_{D,21}]. \quad (3)$$

As mentioned above, $[S_s]$ should be diagonal, which implies that $[S_{D,21}]$ must diagonalize $[S]$. This can be accomplished if we choose

$$[S_{D,21}] = [Q] \Rightarrow [S_s] = [\Gamma] = \text{diag}\{\gamma_1, \gamma_2, \dots, \gamma_M\} \quad (4)$$

in which the matrix $[Q]$ is composed from the *eigenmodes* of the antenna array arranged in columns. Once $[S_s]$ is diagonal, $[Z_s]$ is diagonal as well, due to the relationship

$$[Z_s] = Z_0 ([U] - [S_s])^{-1} ([U] + [S_s]) \quad (5)$$

in which $[U]$ is the identity matrix and Z_0 is the characteristic impedance of the ports.

The suggested decoupling network is reciprocal and lossless. Its input and output ports are matched and decoupled. The power is transferred according to the matrix of the eigenmodes $[Q]$. Each of the input ports excites a different eigenmode such that every excitation is a superposition of the orthonormal eigenmodes. The input ports are now independent of each other, and this allows matching the ports individually with a self-matching network.

Such a network can be implemented in software at the baseband layer by connecting the array to a computer, which performs the matrix calculations and fulfills the network's designation. However, this implementation is narrowband because of the time delays involved in the calculations, which become significant when working at high frequencies.

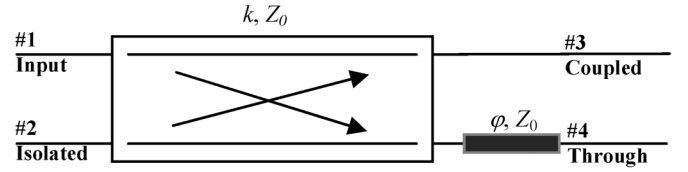


Fig. 3. 180° directional coupler connected to a transmission line with an electrical length φ .

III. HARDWARE IMPLEMENTATION OF THE DECOUPLING NETWORK

A wider bandwidth alternative to the software implementation is hardware implementation of the decoupling network in the RF layer. The implementation of the decoupling network for an M -port array is based on the solution for a 2-port array, in which a 180° directional coupler is connected in tandem with a transmission line with electrical length φ [2]. This can be described by the scattering matrix

$$[S_{\text{coupler}}] = e^{-j\theta} \times \begin{pmatrix} 0 & 0 & k & e^{-j\varphi} \sqrt{1-k^2} \\ 0 & 0 & \sqrt{1-k^2} & ke^{-j(\varphi+\pi)} \\ k & \sqrt{1-k^2} & 0 & 0 \\ e^{-j\varphi} \sqrt{1-k^2} & ke^{-j(\varphi+\pi)} & 0 & 0 \end{pmatrix}. \quad (6)$$

The directional coupler and the transmission line are schematically represented by Fig. 3.

Such a directional coupler is able to decouple a 2-port array by choosing proper values for k , φ , and θ .

A general method to decouple an arbitrary M -port array was developed by Geren *et al.* and is described in [3]. It is based on diagonalizing the imaginary part of $[Z]$, compensating it at each port with a serial imaginary impedance, followed by the diagonalization of its real part and matching it. Each of these diagonalizing matrices is real, and therefore can be factored into $M(M-1)/2$ submatrices, using Givens rotations [3]. Each one of these simple submatrices can be represented by the scattering matrix of a directional coupler, the parameters of which can be derived from the comparison between each of the matrices and the general matrix shown in (6). In our case ($M = 8$), using this method would result in two subnetworks of $(8*7)/2 = 28$ cascaded couplers, compensating both the real and imaginary parts of $[Z]$. This procedure results in 56 couplers for the whole decoupling network. As one can observe, this implementation is very complicated and inapplicable for large arrays.

In the present work, a different approach is adopted [5]. It involves a combination of the method mentioned above and the method described in [2]. The suggested method uses the symmetry planes in the array to divide the array elements in symmetrical groups, resulting in decoupling between these groups. In our case, a symmetric rearrangement of the elements (which is realized by renumbering them) leads to a new indexing as shown in Fig. 4.

The horizontal symmetry plane divides the array into two groups so that the element i is symmetric to the element $4 + i$ ($1 \leq i \leq 4$) in terms of the same scattering parameters. Every symmetrical pair of elements needs to be connected by a 3-dB 180° coupler [the scattering matrix of which is derived

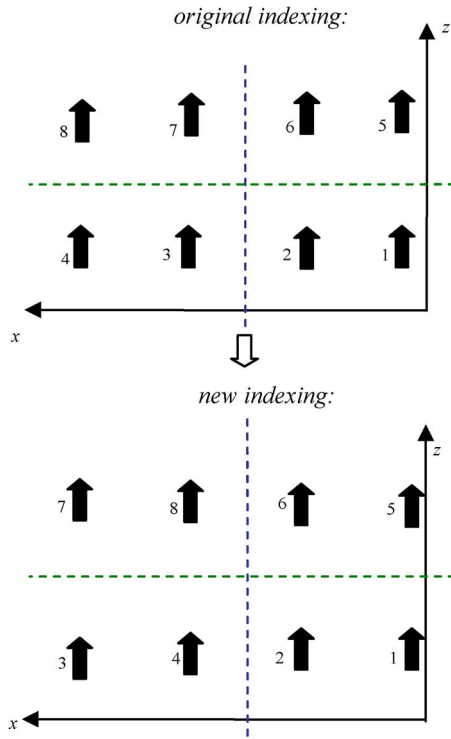


Fig. 4. Suggested array's symmetry planes along with the element indexing: original and new.

by substituting $k = 1/\sqrt{2}$, $\varphi = 0$, and $\theta = \pi/2$ in (6)]. As a result of the connection of these four hybrids (which constitutes the first layer of the decoupling network), there will be no coupling between the elements 1–4 and 5–8.

The vertical symmetry plane divides each of the two groups mentioned into two subgroups so that the element i is symmetric to the element $2 + i$ ($1 \leq i \leq 2$, $5 \leq i \leq 6$). Again, every symmetrical pair of elements needs to be connected by a 3-dB 180° coupler. After the connection of these four couplers (which constitutes the second layer of the decoupling network), there will be no coupling between the elements 1–2, 3–4, 5–6, and 7–8.

At this point, there are no more symmetry planes left, so this method is exhausted. In order to continue the process, which requires the decoupling of the elements of each foursome, the first method [3] is used. As discussed, the decoupling of two elements requires $2 * (2 * 1) / 2 = 2$ cascaded directional couplers. The connection of all the described layers together produces a decoupling network, which consists of 16 directional couplers in comparison to 56 couplers needed if the symmetry planes are not taken in consideration. The impedance matrix at the input ports of the network is diagonal and real, which means that matching can be easily performed at each port independently (for example, with $\lambda/4$ transformers, or with real impedances). The whole network is shown in Fig. 5.

The benefits of working with the decoupling network can be seen in Fig. 6, which shows the dependence of the reflection coefficient on the scanning angle at the ports of the lower-right quartet (ports 1, 2 according to the original indexing in Fig. 4), for a predefined current distribution (Bayliss–20 dB sidelobe level (SLL) and $\bar{n} = 10$).

One can observe that, without the decoupling network, the reflection coefficient varies significantly at each port, producing

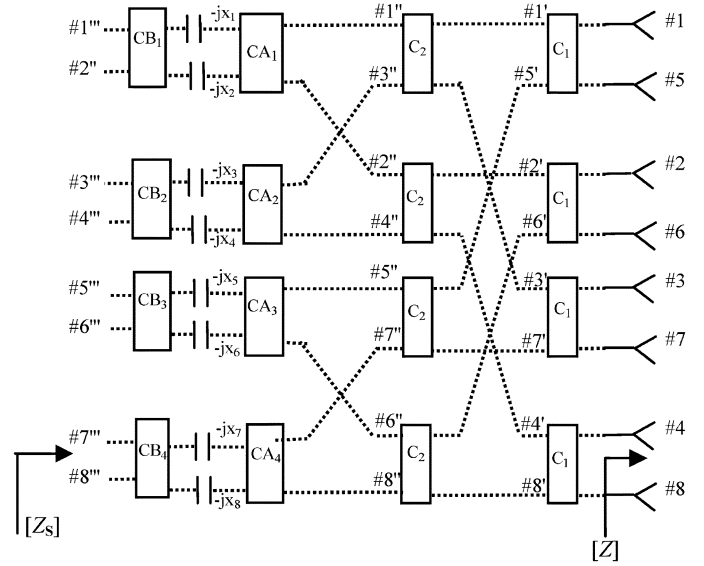


Fig. 5. Decoupling network (antennas: #1–8; input ports: #1''–8'''). Each rectangle represents a directional coupler. More about the scattering matrices of the couplers and the way they are connected can be found in [2] and [3], along with the theory leading to it. The impedance matrix at the input ports $[Z_S]$ is diagonal, while the impedance matrix $[Z]$ at the antennas terminals is a full 8×8 matrix.

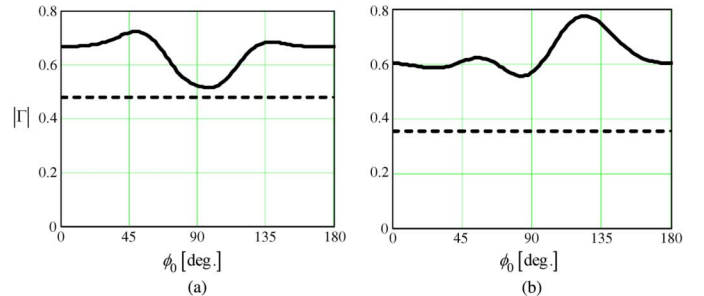


Fig. 6. Dependence of the reflection coefficient $|\Gamma|$ on the scanning angle ϕ_0 for Bayliss distribution with SLL = -20 dB and $\bar{n} = 10$ at ports (a) #1 and (b) #2; (—) without the decoupling network; (----) with the decoupling network.

different return losses as a function of the scanning angle. A similar dependence occurs for other current distributions as well. On the other hand, when the decoupling network is used, a constant reflection coefficient is obtained at each port, which allows independent matching with respect to other ports. This is the significance of the decoupling network, and it demonstrates the necessity of such a network for antenna arrays.

In reality, the directional couplers used for the decoupling network implementation are lossy. In such an instance, the coupler scattering matrix described in (6) changes to reflect finite return loss at all input ports and finite coupling between the isolated ports. Given that the coupler is symmetrical, we can assume without loss of generality that $S_{11} = S_{22} = S_{33} = S_{44}$ and $S_{12} = S_{21} = S_{34} = S_{43} = D$. Accordingly, the new coupler scattering matrix is

$$[S_{\text{coupler}}] = e^{-j\theta} \times \begin{pmatrix} S_{11} & D & k & e^{-j\varphi}\sqrt{1-k^2} \\ D & S_{11} & \sqrt{1-k^2} & ke^{-j(\varphi+\pi)} \\ k & \sqrt{1-k^2} & S_{11} & D \\ e^{-j\varphi}\sqrt{1-k^2} & ke^{-j(\varphi+\pi)} & D & S_{11} \end{pmatrix}. \quad (7)$$

TABLE I
COMPARISON OF THE COUPLING VALUES OF THE COUPLERS IN THE DECOUPLING NETWORK BEFORE AND AFTER THE GA OPTIMIZATION

	C_1	C_2	CA_1	CA_2	CA_3	CA_4	CB_1	CB_2	CB_3	CB_4
before GA	0.707	0.707	0.924	0.71	0.896	0.765	0.958	-0.968	-0.921	0.979
after GA	0.732	0.654	0.972	0.884	0.954	0.961	-0.975	-0.95	-0.975	-0.783

Consequently, the new structure of the decoupling network described in (2) transforms to

$$[S_D] = \begin{pmatrix} [S_{D,11}] & [S_{D,21}]^T \\ [S_{D,21}] & [S_{D,22}] \end{pmatrix} \quad (8)$$

and the total system scattering matrix given in (3) changes to

$$[S_S] = [S_{D,11}] + [S_{D,21}]^T [S] ([U] - [S_{D,22}] [S])^{-1} [S_{D,21}]. \quad (9)$$

One can easily show that (9) reduces to (3) for a lossless network. Given the scattering matrix of the system, the currents \mathbf{I} at the input ports of the antenna elements can be related to the incident waves \mathbf{a}_s of the entire system through

$$\mathbf{I} = \frac{1}{Z_0} ([U] - [S]) ([U] - [S_{D,11}] [S])^{-1} [S_{D,21}] \mathbf{a}_s. \quad (10)$$

To check the effect of a lossy decoupling network on the decoupling network performance, typical directional couplers with $S_{11} = -20$ dB and $D = -24$ dB were considered. The array parameters were the following: operating frequency 10 GHz, dipole length 1.5 cm, dipole radius 0.29 mm, $d = 1.5$ cm, $h = 0.75$ cm. For simplicity, the excitation vector \mathbf{a}_s for the entire system was chosen to be uniform. To compensate for the errors caused by the assumption of finite S_{11} and D , a genetic algorithm (GA) [6] was used to change the coupling parameters (amplitude and phase) of the couplers in the decoupling network shown in Fig. 5. The cost function goal of the GA was minimization of all off-diagonal members of the system impedance matrix $[Z_s]$. The parameters of the GA were the following: population 200, crossover at 60% and 5% mutation. Table I shows a comparison of the network coupling values of the network directional couplers before and after the GA optimization. C_1, C_2, CA_i, CB_i ($i = 1 \div 4$) are the coupling values of the couplers shown in Fig. 5.

Fig. 7 shows a comparison in the H-plane ($\theta = \pi/2$) radiation patterns of an ideal 2×4 array (no coupling among elements), an array with coupled elements, an array with a lossy decoupling network, and an array with a GA optimized lossy decoupling network. In the cases of the lossy and optimized lossy decoupling networks, the scattering matrices $[S_D]$ and $[S_s]$ have been computed using (8) and (9), respectively, and validated by simulation of the decoupling network shown in Fig. 5 using the commercial software ADS. Given $[S_D]$, the currents of the array elements were computed using (10) and the corresponding array radiation patterns as described in [4]. One can observe a significant degradation in the radiation pattern for a lossy decoupling network compared to a lossless network and the significance of the optimization procedure to compensate it.

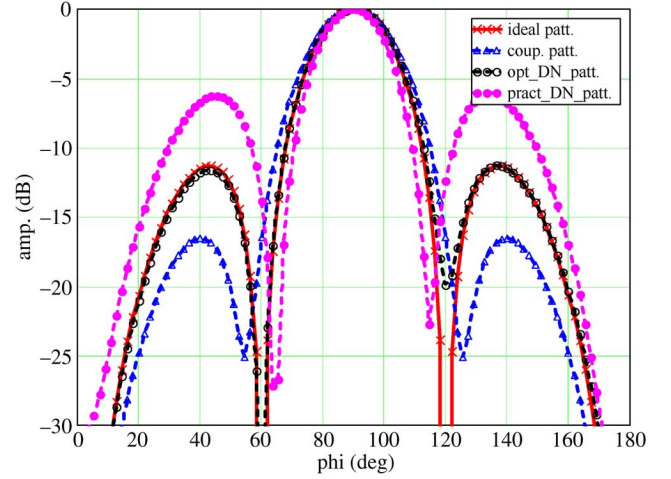


Fig. 7. H-plane ($\theta = \pi/2$) radiation patterns of a 2×4 array without coupling (ideal patt.), array with coupling (coup. patt.), array with real components decoupling network (pract_DN_patt.), and an array with optimized real decoupling network (opt_DN_patt.).

IV. CONCLUSION

This letter has demonstrated a new approach for designing and implementing a decoupling network for a large antenna array based on a combination of two existing methods, which results in significant hardware savings: 16 couplers instead of 56 in the general method (a ratio of 1:4) described in [3]. Such savings increase for large arrays. A GA was used to change the elements to compensate for the degradation in performance in a lossy decoupling network.

The suggested approach can be generalized for other cases as well—different array elements, different geometric structures (such as triangular, rectangular, or circular grids).

REFERENCES

- [1] H. Steyskal and J. S. Herd, "Mutual coupling compensation in small array antennas," *IEEE Trans. Antennas Propag.*, vol. 38, no. 12, pp. 1971–1975, Dec. 1990.
- [2] C. Volmer, J. Weber, R. Stephan, K. Blau, and M. A. Hein, "An eigenanalysis of compact antenna arrays and its application to port decoupling," *IEEE Trans. Antennas Propag.*, vol. 56, no. 2, pp. 360–370, Feb. 2008.
- [3] W. P. Geren, C. R. Curry, and J. Andersen, "A practical technique for designing multiport coupling networks," *IEEE Trans. Microw. Theory Tech.*, vol. 44, no. 3, pp. 364–371, Mar. 1996.
- [4] R. S. Elliott, *Antenna Theory and Design*. Englewood Cliffs, NJ: Prentice-Hall, 1981.
- [5] E. Rivkin and R. Shavit, "An efficient decoupling feeding network for phased arrays," in *Proc. COMCAS Int. Symp.*, Tel-Aviv, Israel, Nov. 2009, pp. 183–189.
- [6] D. E. Goldberg, *Genetic Algorithms*. Reading, MA: Addison-Wesley, 1989.